



INVESTIGATING COUNTER-ROTATING OPEN ROTOR NOISE SOURCES FROM A BROADBAND POINT OF VIEW

Csaba Horváth¹

¹Department of Fluid Mechanics, Budapest University of Technology and Economics (BME)
Bertalan Lajos utca 4-6, 1111, Budapest, Hungary

ABSTRACT

In an attempt to lower the noise level of counter-rotating open rotors, phased array microphone measurements and state-of-the-art beamforming technology have recently been implemented in their investigation. The results are very useful, though initially misleading and difficult to comprehend. Recent publications have helped explain beamforming results of rotating coherent noise sources, typical tonal noise sources for counter-rotating open rotors. Building on the former results, the present beamforming investigation provides a novel approach for identifying broadband noise sources of counter-rotating open rotors. The method pinpoints dominant broadband noise sources to given areas of the rotor surface, and also helps separate out a noise source associated with shaft orders which result from blade nonuniformities, such as measurement instrumentation mounted on the rotor surface, which could otherwise be mistakenly associated with the tonal or broadband noise sources.

1 INTRODUCTION

As a result of the increased fuel prices of the 1970s and 1980s, open rotor propulsion systems were investigated as a possible means by which to reduce the fuel burn of aircrafts while maintaining similar cruise speeds to that of turbofan aircrafts. [1, 2] There are many questions and concerns with regard to the implementation of open rotor technology, which were investigated, but only partially resolved during these tests. One of these concerns was the challenge of reducing the noise of Counter-Rotating Open Rotor (CROR) engines in order to meet noise regulations, while maintaining the aforementioned advantageous propulsive efficiency. The interest in a radically new engine technology, such as open rotor propulsion systems, diminished as fuel prices fell and therefore the research and development programs of the 1980s were ended. A renewed interest in highly efficient propulsion systems has been triggered by rising fuel prices, as well as the increasingly stringent limitations regarding aircraft greenhouse-gas emissions and noise, which have led designers of modern aircraft engines back to the further investigation of open rotor propulsion systems. [3]

In the early testing of CROR propulsion systems, many parameters were investigated in order to better understand the noise production mechanisms and to test noise reduction concepts. These included inter-stage spacing, [2] pylon and fuselage effects, [4] angle-of-attack (AOA) effects, [5] advanced blade designs including blade sweep, [6] and reduced aft rotor diameter. [7] These investigations resulted in many questions being answered and challenges being solved, while also formulating new ones. With the help of many state-of-the-art technologies, which were not yet available during the time of the previous investigations, it is believed that the present tests and simulations will help in resolving these remaining questions and challenges and in making the widespread use of open rotor propulsion systems a reality in the near future.

In the 1980s, wind tunnel acoustic investigations of CROR were done using single microphones and arrays of microphones, which were fixed, or traversed along the sideline or around the circumference of the measurement rig. The signals of the various microphones were individually processed, giving information as to the directivity and the spectral content of the signals. [2] Today, state-of-the-art beamforming technology has made phased array microphone measurements of complex aeroacoustic phenomena a realizable task, by which the localization of noise sources is possible. [8] The first published phased array microphone measurements of a CROR describe results attained using a linear microphone array. [9] These results evaluate the noise source levels as a function of the axial source position, as well as giving emission angles for the broadband noise as a function of the axial source position. Planar microphone array results were first presented in 2013, when Kennedy et al. investigated the installation effects of CROR on multiple aircraft configurations, [10, 11, 12] and Horváth et al. investigated isolated CROR, localizing rotating coherent CROR noise sources to the Mach radius. [14] The investigation of Horváth et al. showed that the results of planar phased array measurements of CROR can be misleading, locating rotating coherent noise sources at their respective Mach radii rather than the source of the noise.

The investigation of the broadband noise of CROR was not a main goal of the early research done on the subject. At the time all efforts were focused on lowering the noise level of the predominant Blade Passing Frequency (BPF) and interaction tones in order to meet noise regulations. As advanced CROR designs have managed to significantly lower tonal noise levels, the importance of understanding, localizing and eliminating broadband noise sources has been realized. [14, 15, 16] Prior to this investigation, the few results published on the broadband noise of CROR have introduced predictive schemes, [15, 16] have presented results of linear microphone array measurements, determining emission angles for broadband noise as a function of the axial source position, [9] and have investigated the broadband noise of installed CROR using planar phased arrays. [11]

The results presented herein advance the state of the art of open rotor technology by introducing a novel approach for investigating the broadband noise sources of an uninstalled CROR with a planar microphone array positioned broadside and parallel to the axis of the CROR. Two test cases are presented, demonstrating how useful these evaluation methods are in localizing broadband noise sources on the rotor surface, identifying those noise generation mechanisms which should be dealt with in order to most effectively reduce the broadband noise of CROR. In addition, tonal noise source investigations pertaining to the same configurations have shown cases where a noise source other than the expected BPF or interaction tone dominate certain frequency bins. [13] This study identifies the origin of these particular noise

sources, showing yet another instance where beamforming proves to be useful in identifying the true noise sources of CROR.

2 MEASUREMENT SETUP

In the framework of the present collaboration between NASA and General Electric (GE), investigating the design space for lowering noise while maintaining the high propulsive efficiency of open rotor propulsion systems, extensive testing of the F31/A31 Historical Baseline Blade Set, with regard to aerodynamic performance, acoustic characteristics and detailed flow field features, was conducted on the Open Rotor Propulsion Rig (ORPR) in the NASA Glenn Research Center 9' x 15' Low Speed Wind Tunnel (LSWT). Details regarding the geometric configuration and the general test setup can be found in [17].

The refurbished ORPR is the same rig which was used during the tests conducted by NASA and GE in the 1980s. The ORPR provides an opportunity for independently setting the rotational speeds, as well as the blade angles of the two individual rotors. The ORPR is mounted on a turntable which allows for the investigation of AOA effects, and a pylon can also be mounted upstream of the rotors, in order to investigate installation effects. Details regarding the ORPR can be found in [17] and [6].

The F31/A31 Historical Baseline Blade Set was used during these tests. F and A refer to the forward and aft rotors, respectively, and will also be used as subscripts in the text. The forward rotor has 12 blades, while the aft rotor has 10 blades. Details regarding the blade set can be found in [17].

Regarding the phased array portion of the tests, they were conducted in the LSWT, with the phased array being installed in a cavity along the Southern wall of the facility, directly across from the ORPR. The array was recessed into the cavity, leaving a gap between the array plate and the Kevlar® which was tightly stretched over the cavity. In this way, the plate of the array was located 1.597 [m] (62.875") from the center plane of the ORPR for 0° Angle-Of-Attack (AOA). Figure 1 shows the ORPR and the phased array, as positioned in the tunnel wall of the LSWT. No traversing of the phased array was attempted. The array was recessed into the cavity in order to remove the boundary layer flow and hence the boundary layer noise from its surface. The Kevlar® sheet was utilized in order to provide a smooth aerodynamic surface for the flow, while also being acoustically transparent for the array. This technique has been tested and applied by Jaeger et al. [18] The phased array microphone system used for the tests is the Optinav Array48. The microphone array consists of 48 Earthworks M30 microphones, which are built into a precision machined aluminum tooling plate. An optical camera is also built into the aluminum plate.

Many test configurations were run in the given test matrix, giving an opportunity for multiple comparisons. The configurations which were tested are the following:

- Rotors: F31/A31 vs. blades off
- Pylon vs. no pylon
- Takeoff nominal vs. approach blade angle settings
- AOA: 0°, -3° and -8°
- Ma: 0.2 (investigated for all cases), 0.22 (investigated for some cases at 0° AOA), 0.05, 0.1, 0.15, 0.18, 0.2, 0.22 and 0.229 (investigated during the blades off runs)

- Rotor RPM: Multiple settings, ranging from windmilling to 7487 RPM (values are corrected to standard day)

Measurements were made for all the cases which can be combined from the above mentioned parameters, with the sampling time and sampling frequency of each measurement being 45 [s] at 96 [kHz].

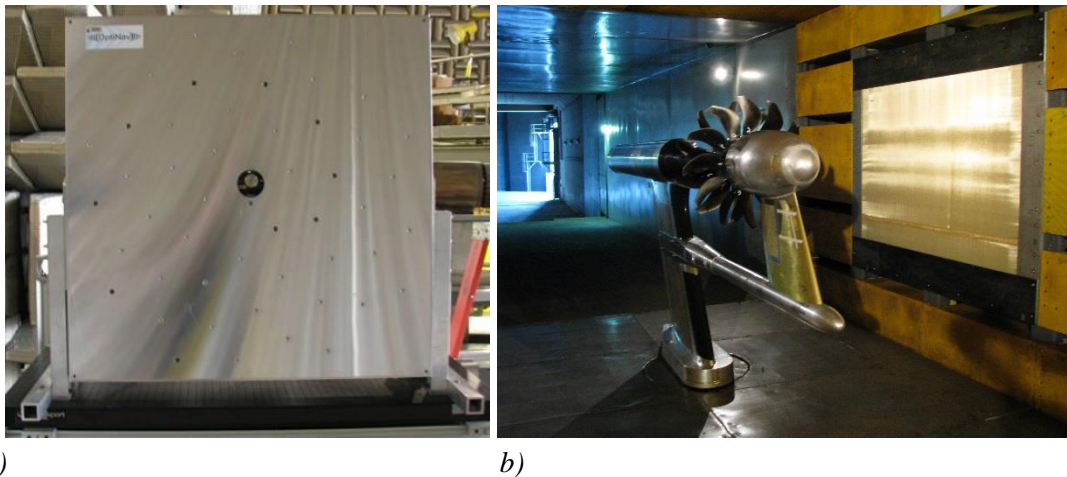


Fig. 1. a) Close-up view of the Array48 system b) Array installed behind the Kevlar® window.

The configurations to be investigated here are the takeoff nominal and approach, with the takeoff nominal and approach blade angle settings being examined at the design point. Here no pylon or AOA effects will be considered. The design takeoff nominal condition for the F31/A31 blade configuration consists of the F31/A31 blade angle settings of $40.1^\circ/40.8^\circ$, respectively, a wind tunnel Ma of 0.2 and a corrected standard day RPM of 6450 RPM for both rotors. The design approach condition for the F31/A31 blade configuration consists of the F31/A31 blade angle settings of $33.5^\circ/35.7^\circ$, respectively, a wind tunnel Ma of 0.2 and a corrected standard day RPM of 5598 RPM for both rotors.

3 PROCESSING OF THE RESULTS

All data sets are processed using order analysis, aligning the BPF signals, their harmonics and the interaction tones of the various instances, making the processing, presenting and comparison of the data sets easier. As a result of this, the bandwidths of the bins do not agree with conventional bandwidths, but are determined individually for each case by dividing the frequency range between two harmonics of the BPF of the aft rotor (BPF_A) into 50 equal bins.

Prior to processing all the data, tests were done to determine which methods should be applied in order to provide a basic, yet complete and accurate set of results. These tests investigate aspects which could influence the investigation and the results, such as how well the various beamforming and deconvolution methods resolve the data, how long these methods take, whether the applied transform length is sufficient, what frequency range should be investigated, whether the placement of the region of interest on the individual blades makes any difference when varying the AOA, as well as the effect of the Kevlar® window, to name a few.

It can be seen in Fig. 1, that a sheet of Kevlar® is stretched over the phased array, the array being recessed into the wall of the wind tunnel. As discussed earlier, the Kevlar® provides a smooth aerodynamic surface for the flow going through the tunnel, removing the boundary layer flow from the surface of the array, while also providing an acoustically transparent surface through which the acoustic waves coming from the ORPR can reach the microphones. In this way the signal-to-noise ratio at the microphones is improved, which leads to the improvement of the dynamic range of the results. [18] For all the results presented here, the use of a Kevlar® window, the removal of the diagonal of the cross-spectral matrix, and a long sampling time are applied in order to increase the dynamic range and remove the self-noise from the results. The microphone signals therefore experience some modest attenuation, but a much cleaner beamforming map, with a large dynamic range, can be reached.

The above mentioned investigation results show that applying certain beamforming and deconvolution methods, useful results can be attained when examining a specific frequency range and bandwidth. The disadvantage of using deconvolution methods, as compared to classical beamforming methods, is that much more time is necessary for evaluating the results, and that various methods only provide cleaner results for limited frequency and bandwidth ranges, while none of the deconvolution methods looked at provide results which are universally optimal. The experienced eye, on the other hand, can, in most instances examined here, separate the real results from the sidelobes produced using the classical time-domain and frequency domain delay-and-sum beamforming methods. Delay-and-sum beamforming in the frequency domain was therefore applied in all cases, providing a useful set of basic results for all the test cases and frequency ranges to be examined in a finite amount of time. The examined plane used throughout this study was the vertical plane that is parallel to the microphone array and passes through the axis of the ORPR. The cross-spectral matrices created during the processing of the data were made using a transform length of 4096, with 6 [dB] being subtracted from the results to account for the pressure doubling at the phased array plate surface.

4 BROADBAND NOISE SOURCES

The literature provides information regarding the noise source mechanisms responsible for the broadband noise of CROR. Being that this investigation looks at uninstalled CROR, an emphasis is placed on relevant noise sources. For the most part, CROR broadband noise sources are sorted into three main groups, as seen in [15, 19, 20], namely leading edge noise sources, trailing edge noise sources, and blade tip noise sources. Though multiple names are used for the given noise sources, these were used here as they are intuitive for locating the noise sources seen on beamforming maps.

The leading edge noise sources refer to broadband noise sources which result from the interaction of nonuniform turbulent inflow with a rotor blade. [15, 19, 20] The noise level depends on the magnitude of the inflow turbulence, being quite significant for high turbulence at low speed, such as takeoff and approach conditions. [19] According to [19], the noise sources should be localized to the leading edge for high frequency cases where the wavelength is smaller than the blade chord, but could be located along the entire blade chord for low frequencies, where the blade can be considered as a compact noise source. The source of the nonuniform turbulent inflow can vary, with typical examples for uninstalled CROR being atmospheric turbulence ingestion, [15, 20] the rotor-wake of the upstream rotor, [15, 20] and

the turbulent blade tip vortex of the upstream rotor. [15] Being that modern designs, including the F31/A31 blade set, have cropped aft rotors in order to avoid the impingement of the blade tip vortex with the aft rotor, it is expected that this final noise source should be irrelevant.

Trailing edge noise, otherwise known as boundary layer self-noise or rotor self-noise, occurs when the turbulent boundary layer developing on a blade surface passes over the trailing edge, resulting in fluctuating blade loading. [15, 19, 20]

Blade tip noise, also called vortex self-noise, occurs as the turbulence in the core of the blade tip vortex interacts with the rotor blade. [19, 20] According to [19], this occurs as the blade tip vortex interacts with the trailing edge.

The literature states, as can be seen in typical CROR spectrums, that the relative impact of broadband noise on the noise level increases at higher frequencies, as the amplitudes of tonal noise sources decrease and are buried in the broadband noise. [14] It can also be seen in the results of [9], that the maximum levels of broadband noise can be measured in the lateral direction, where the microphone array of the present investigation is positioned.

5 RESULTS

5.1 Removing tonal noise sources

Evaluating the results, the dominant noise sources of a given frequency bin are examined by investigating the largest noise sources that are located on the beamforming maps (referred to as beamform peaks) which depict the areas to which the noise sources are localized by the beamforming process together with the beamform peak Power Spectral Density (PSD) spectrum. The combined use of the PSD spectrum and the beamforming maps is useful for recognizing the trends occurring in the results. Figure 2 presents results for the takeoff nominal BPF of the forward rotor (BPF_F) tone. In this figure, as in similar figures to be presented later, the left half shows the PSD spectrum, while the right half shows the beamforming map for the examined frequency bin, marked in the PSD spectrum with a black asterisk. It can be seen that the beamforming process localized the noise source outboard of the forward rotor blade tip, at the Mach radius.

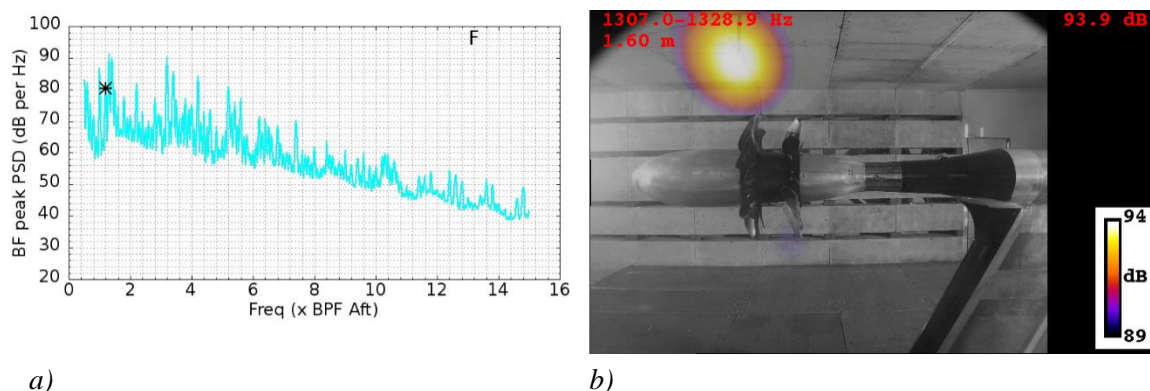


Fig. 2. Beamforming results for the takeoff nominal BPF_F tone. a) PSD spectrum b) beamforming map.

In preparing the results for the investigation of the broadband noise sources, the first step is to remove all the beamforming maps from the complete stack of the spectrum which point to known tonal noise sources. In light of the results presented in [13], this is done by removing all beamforming maps which localize the noise sources to their respective Mach radii. All other beamforming maps, regardless of whether they belong to a frequency bin which is expected to be tonal or broadband, are left in the stack. It should be mentioned that as a result of the finite resolution of the time series and the Fourier transform applied in processing the results, the tonal peaks of the spectrum are not sharp and therefore a few bins on either side of a given peak also need to be removed when removing tonal noise sources, if the noise sources in those bins are also localized to the investigated Mach radius. It should also be mentioned in order to avoid confusion that the sections of the spectrum associated with the removed beamforming maps are not modified in the remaining stack in order to reflect the removal of bins.

5.2 Evaluation of the shaft order noise sources

Investigating the PSD spectrum peaks that remain in the stack after removing the tonal noise sources, such as the one in Fig. 3, which shows the results for a takeoff nominal shaft order, also referred to in the literature as multiple pure tones, it can be seen that not only the broadband noise sources remain in the results. The frequency investigated in the figure is associated with a shaft order that is not removed. The spectrum shows a peak which rises out of the broadband, while the noise source appearing in the beamform map is not located at the Mach radius of the tone. During the investigation of CROR tonal noise sources, the investigations are limited to rotating coherent noise sources, for which, as described in [13], the propagation of the sound waves away from the model coupled with the rotation of the coherent noise sources about an axis results in the phased array locating the noise sources at their respective Mach radii. It is given in [13], that the beamforming process will locate the noise sources of CROR at their actual source locations rather than the Mach radii in cases such as incoherent noise sources and rotating broadband noise sources, in other words for all cases other than rotating coherent noise sources that can be located by applying beamforming under normal conditions. Investigating all peaks in the PSD spectrum remaining after the removal of those which are localized to their respective Mach radii, it is found that they are all shaft orders and that they are all localized to a noise source appearing on the pressure side of the aft rotor near the blade tip. In the literature, Woodward states that earlier experiences have shown that shaft order tones appear in CROR spectrum when blade nonuniformities are present as a result of measurement instrumentation being mounted on the blades. [2] It has been confirmed that instrumentation was mounted during portions of the testing in the vicinity of the noise source which was found using beamforming, but it has not been confirmed whether the sensors were mounted during these particular runs. It appears that a noise source was correctly localized to this area instead of the Mach radius, as some nonuniformities could be present on the blade surface, be that due to currently mounted sensors, or sensors which were previously mounted.

The results explain why the noise sources of certain harmonics of the BPF and interaction tones were not located at their respective Mach radii. An example of this can be seen in Fig. 4, which presents results for the takeoff nominal 2BPF_F tone, which would be expected to be located off the aft rotor at its Mach radius, the same as the BPF_F seen in Fig. 2, but is instead located at the above mentioned position associated with the measurement instrumentation.

Investigations into this instance show a weaker noise source also appearing at the Mach radius of the tone, but the noise source is so weak that it does not appear in the beamforming map as a result of the applied dynamic range.

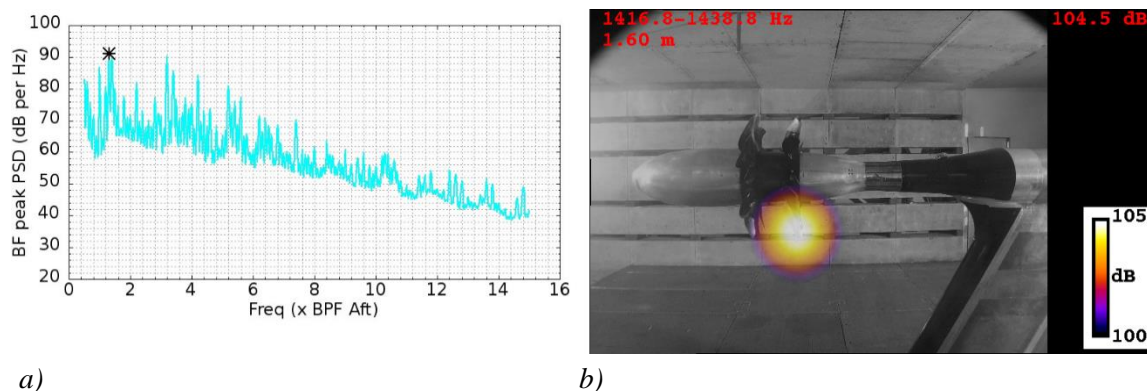


Fig. 3. Beamforming results for a takeoff nominal shaft order. a) PSD spectrum b) beamforming map.

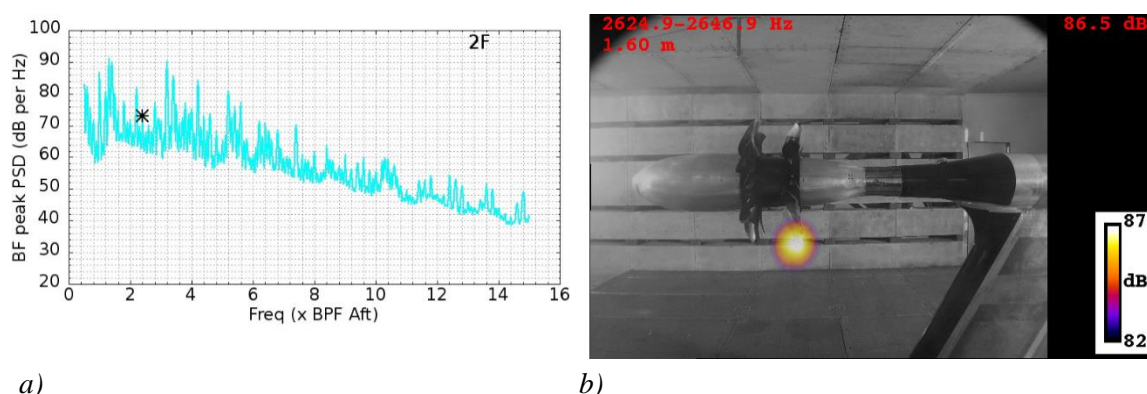


Fig. 4. Beamforming results for the takeoff nominal $2BPF_F$ tone. a) PSD spectrum b) beamforming map.

Though measurement data used to investigate broadband noise would customarily be processed in order to provide results in octave bands or one-third octave bands, it has been decided to use this format during this investigation in order to take advantage of the benefits of order analysis, which proves useful, as the noise sources which dominate over the expected BPF and interaction tone noise sources can therefore be identified. The localization of the noise source of the shaft orders is significant, as it shows another instance where beamforming is very useful in identifying the true noise sources of turbomachinery. Without these beamforming results, the source of the noise would be unknown and it would misleadingly be associated with either the broadband or the rotating coherent tonal noise sources of CROR.

5.3 Evaluation of the broadband noise sources

The beamforming maps remaining after the removal of the rotating coherent tonal noise sources and the affected shaft orders provide information about the broadband noise sources. In this section the various broadband noise sources discussed in earlier sections are identified on the beamforming maps, with typical examples given for each. Analyzing the beamforming

maps, it should be kept in mind that sidelobes appear in the results, and therefore only the larger peaks should be concentrated on, as only those provide relevant information. Being that CROR broadband noise sources are rotating incoherent noise sources, the noise sources to be investigated here are expected to appear at their actual radial and axial positions, as they do.

Investigating the leading edge of the aft rotor, a leading edge broadband noise source is identified. At lower frequencies the noise source appears on the suction side of the rotor, as can be seen in Fig. 5, presenting an example for approach leading edge broadband noise at low frequency. At higher frequencies the noise source is localized to the leading edge of the blade, as can be seen in Fig. 6 and Fig. 7. Figure 6 shows an approach leading edge broadband noise source which can be seen along the leading edge above the axis, while Fig. 7 shows a takeoff nominal leading edge broadband noise source which can be seen along the leading edge below the axis. The noise source discussed here is identified as a leading edge broadband noise source for many reasons. The literature states that leading edge noise sources are resulting from the interaction of a nonuniform turbulent inflow with a rotor blade, [15, 19, 20] with higher frequency (short wavelength) sources being localized to the leading edge of the rotor while low frequency (long wavelength) sources can be located along the entire blade. [19] The measurement results present a transition from the suction side of the aft rotor at low frequencies to the leading edge of the same rotor at high frequencies, as would therefore be expected. It should be mentioned that delay-and-sum beamforming might also play a role in the difficulty of localizing the noise source to solely the leading edge, as the method provides a relatively large noise source for low frequency beamforming maps. In determining the source of the inflow turbulence, it is found to be associated with the wake of the forward rotor, as given in [15, 20]. This is supported by the fact that the forward rotor does not show signs of a dominant leading edge broadband noise source, as would be expected, since no pylon, rotor, or other turbulence generation device is located upstream of it. Investigating other possible sources of inflow turbulence, the broadband results do not show signs of a turbulent blade tip vortex from the forward rotor interacting with the blade tip of the aft rotor, [15] as would be expected of the cropped aft rotor. This would appear in the form of a dominant broadband blade tip noise source on the aft rotor, which is not seen.

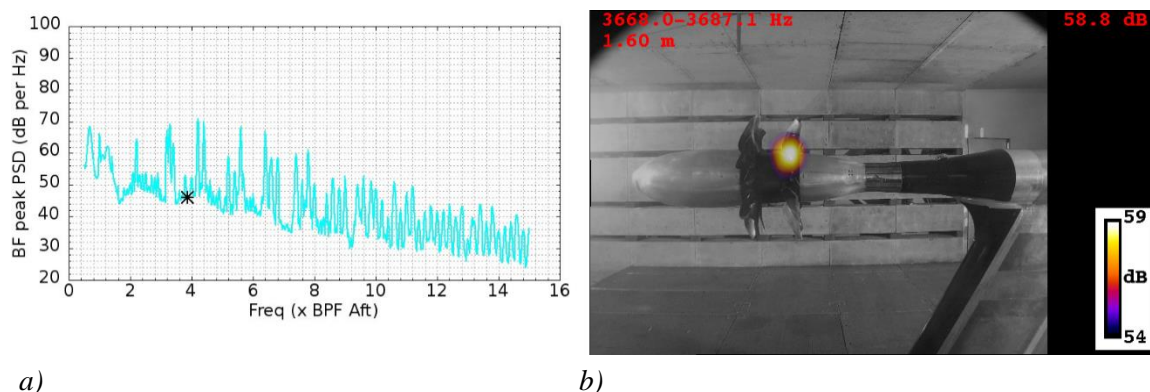


Fig. 5. Beamforming results for the approach leading edge broadband noise source at lower frequencies. a) PSD spectrum b) beamforming map.

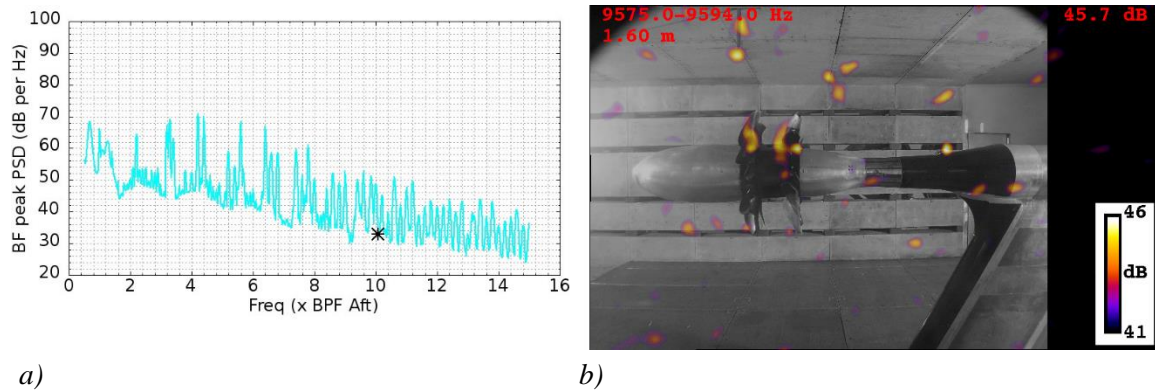


Fig. 6. Beamforming results for the approach leading edge broadband noise source at higher frequencies. a) PSD spectrum b) beamforming map.

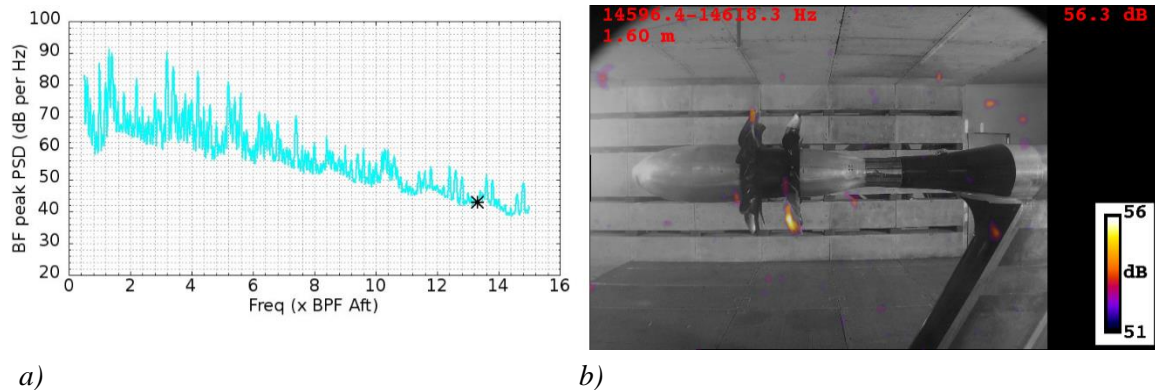


Fig. 7. Beamforming results for the takeoff nominal leading edge broadband noise source at higher frequencies. a) PSD spectrum b) beamforming map.

Unlike leading edge noise sources, trailing edge noise sources are found on both the forward and the aft rotors investigated here. In the results the noise source appears at mid to high frequencies, increasing in significance toward higher frequencies. The trailing edge noise source appearing on the forward rotor can be seen in Fig. 8, which presents a takeoff nominal trailing edge broadband noise source appearing along a large portion of the span of the forward rotor. The reason for associating these noise sources with trailing edge noise comes from the literature, which states that the trailing edge noise generation mechanism is related to the turbulent boundary layer passing over the trailing edge, [15, 19, 20] the noise source here appearing along the trailing edge. The trailing edge noise source is the dominant broadband noise source for the forward rotor. It appears along various portions of the span for different cases, not localizing to only the blade tip or the hub. For the aft rotor, the trailing edge noise source is a weaker noise source that only appears in the beamforming maps if the other noise sources are weak. An example of this can be seen in Fig. 9, where an approach trailing edge broadband noise source can be seen along a large portion of the span of the aft rotor below the axis.

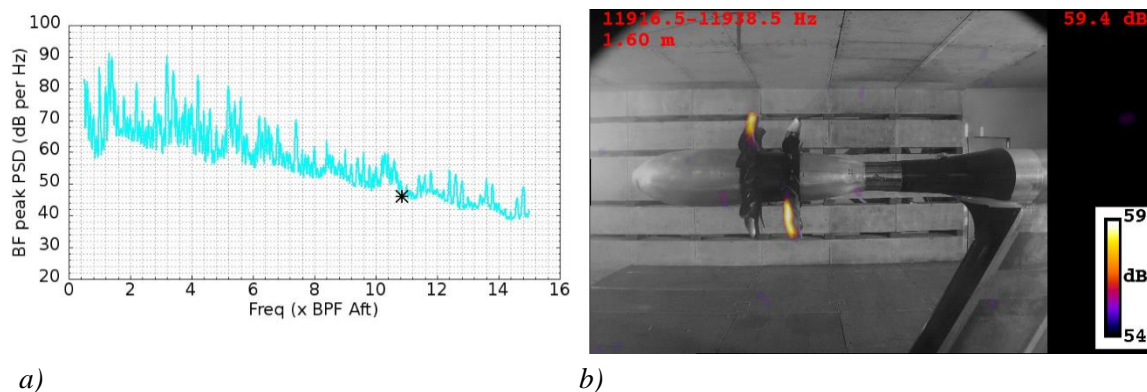


Fig. 8. Beamforming results for the takeoff nominal trailing edge broadband noise source. a) PSD spectrum b) beamforming map.

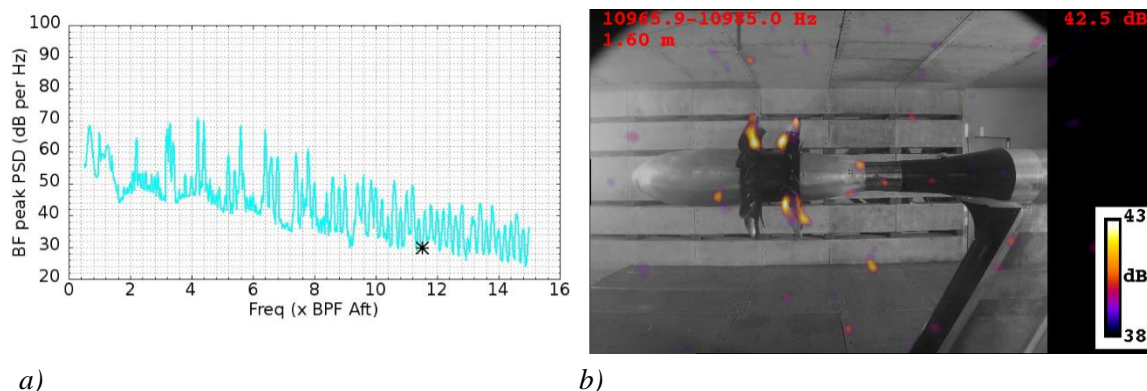


Fig. 9. Beamforming results for the approach trailing edge broadband noise source. a) PSD spectrum b) beamforming map.

The noise sources appearing on the beamforming maps associated with trailing edge noise are not concentrated to the blade tip. They appear along different portions of the span for various instances. Therefore, it is believed that blade tip noise, occurring when the turbulent core of the blade tip vortex interacts with the trailing edge, [19, 20] is not a dominant noise source for the investigated cases.

Summarizing the noise sources identified in this investigation, those appearing at shaft orders and associated with measurement instrumentation are localized to the pressure side of the aft rotor. Leading edge noise sources are localized to the suction side of the aft rotor for low frequencies and to the leading edge of the aft rotor for high frequencies. This noise source is the dominant broadband noise source for both of the cases investigated, appearing at all frequencies above 1BPF_A . Significant leading edge noise sources are not noticed on the forward rotor, but on the other hand trailing edge noise sources are. These are the dominant broadband noise sources of the uninstalled forward rotors investigated here, as seen in the results at mid to high frequencies. Trailing edge noise sources are seen on the aft rotors as well, though these noise sources are relatively insignificant as compared to the other broadband noise sources.

Results for the broadband noise sources of the design takeoff nominal and the design approach conditions of the F31/A31 Historical Baseline Blade Set are presented above. The usefulness of the novel approach for determining the broadband noise sources of CROR is

illustrated through examples, localizing the dominant broadband noise sources to areas of the rotor surface. It is also seen, that without this novel approach, the noise sources associated with the measurement instrumentation would most likely have been deemed as being associated with either the broadband or tonal noise sources.

6 CONCLUSIONS

This paper introduced a series of planar phased array microphone measurements conducted on the F31/A31 Historic Baseline Blade Set in the 9' x 15' LSWT of NASA Glenn Research Center. These CROR beamforming results provide a means for validating research tools, as well as offering the research community a data set for the investigation of CROR. The design takeoff nominal and approach conditions were investigated using a novel approach in analyzing the beamforming results, localizing broadband noise sources of CROR to given sections of the forward and aft rotors. The method advances the state of the art of CROR measurement technique by providing a means by which CROR broadband noise sources can easily be localized, identified, and sorted according to noise generation mechanism. The results were analyzed, setting out broadband noise sources which dominate the sound field of the F31/A31 Historic Baseline Blade Set at design takeoff nominal and approach conditions from other possible broadband noise sources. The results also give an answer as to why certain shaft order peaks in the PSD spectra did not align with their Mach radii in the beamforming maps. The localization of the noise sources of the given shaft orders advances the state of the art of beamforming for turbomachinery by presenting how beamforming can be used to identify the true noise sources in a case where the noise source is neither rotating coherent nor broadband. Without such a beamforming method, the true source of the noise would be unknown and would misleadingly be associated with either the broadband or the rotating coherent tonal noise sources of CROR. The methodologies presented in this investigation will be applied in future studies, comparing the other elements of the test matrix to the design cases presented here.

7 ACKNOWLEDGEMENTS

This testing and research was funded by the Environmentally Responsible Aviation Project of the NASA Integrated Systems Research Program and the Fixed Wing Project of the NASA Fundamental Aeronautics Program. A portion of the study was supported by the Hungarian Fund for Science and Research under contract K 83807, and relates to the scientific program of the projects “Development of quality-oriented and harmonized R+D+I strategy and the functional model at BME” and “Talent care and cultivation in the scientific workshops of BME” under the grants TÁMOP-4.2.1/B-09/1/KMR-2010-0002 and TÁMOP-4.2.2/B-10/1-2010-0009, respectively.

REFERENCES

- [1] M. D. Bowles. “The “Apollo” of aeronautics: NASA's aircraft energy efficiency program, 1973-1987.” NASA Headquarters, Washington, 2010, Chap. 5.
- [2] R. P. Woodward. “Noise of a model high speed counterrotation propeller at simulated takeoff/approach conditions (F7/A7).” NASA TM-100206, 1988.

- [3] N. Peake and A. B. Parry. “Modern challenges facing turbomachinery aeroacoustics.” *Annu. Rev. Fluid Mech.*, Vol. 44, 2012, pp. 227-248. doi: 10.1146/annurev-fluid-120710-101231.
- [4] R. P. Woodward and C. E. Hughes. “Noise of a model counterrotation propeller with simulated fuselage and support pylon at takeoff/approach conditions.” AIAA-89-1143. AIAA 12th Aeroacoustics Conference, San Antonio, 1989.
- [5] R. P. Woodward. “Noise of a simulated installed model counter rotation propeller at angle-of-attack and takeoff/approach conditions.” AIAA-90-0283, 28th Aerospace Sciences Meeting, Reno, 1990.
- [6] R. P. Woodward, D. G. Hall, G. G. Podboy, and R. J. Jeraki. “Takeoff/approach noise of a model counterrotation propeller with a forward-swept upstream rotor.” AIAA-93-0596, 31st Aerospace Science Meeting and Exhibition, Reno, 1993.
- [7] R. P. Woodward and E. B. Gordon. “Noise of a model counterrotation propeller with reduced aft rotor diameter at simulated takeoff/approach conditions (F7/A3).” AIAA-88-0263, 26th Aerospace Sciences Meeting, Reno, 1988.
- [8] T. J. Mueller. “Aeroacoustic measurements.” Springer-Verlag, Berlin, 2002, Chaps. 2.
- [9] S. Funke, L. Kim and H. A. Siller. “Microphone-array measurements of a model scale contra-rotating open rotor in a reverberant open wind-tunnel.” AIAA-2011-2766, 17th AIAA/CEAS Aeroacoustics Conference (32nd AIAA Aeroacoustics Conference), Portland, 2011.
- [10] J. Kennedy, P. Eret, G. Bennett and M. Di Giulio. “WENEMOR: Wind tunnel tests for the evaluation of the installation effects of noise emissions of an open rotor advanced regional aircraft.” AIAA-2013-2092, 19th AIAA/CEAS Aeroacoustics Conference, Berlin, 2013.
- [11] J. Kennedy, P. Eret, G. Bennett, F. Sopranzetti, P. Chiariotti, P. Castellini, A. Finez and C. Picard. “The application of advanced beamforming techniques for the noise characterization of installed counter rotating open rotors.” AIAA-2013-2093, 19th AIAA/CEAS Aeroacoustics Conference, Berlin, 2013.
- [12] J. Kennedy, P. Eret and G. Bennett. “A parametric study of installed counter rotating open rotors.” AIAA-2013-2094, 19th AIAA/CEAS Aeroacoustics Conference, Berlin, 2013.
- [13] Cs. Horváth, E. Envia and G.G. Podboy. “Limitations of phased array beamforming in open rotor noise source imaging.” *AIAA Journal*, accepted for publication, 2014.
- [14] A.B. Parry, M. Kingan and B. J. Tester. “Relative importance of open rotor tone and broadband noise sources.” AIAA 2011-2763. 17th AIAA/CEAS Aeroacoustics Conference, Portland, Oregon, 05-08 June 2011.
- [15] V. P. Blandeau. “Aerodynamic broadband noise from contra-rotating open rotors.” PhD Thesis, University of Southampton, 2011.
- [16] V. P. Blandeau and P. F. Joseph. “Broadband noise due to rotor-wake/rotor interaction in contra-rotating open rotors.” *AIAA Journal*, Vol. 48, No. 11, 2010.

- [17] D. E. Van Zante, J. A. Gazzaniga, D. M. Elliott, R. P. Woodward. “An open rotor test case: F31/A31 historical baseline blade set.” ISABE-2011-1310, 20th International Symposium on Air Breathing Engines, Gothenburg, 2011.
- [18] S. M. Jaeger, W. C. Horne and C. S. Allen. “Effect of surface treatment on array microphone self-noise,” AIAA-2000-1937, 6th AIAA/CEAS Aeroacoustics Conference, Berlin, 2000.
- [19] B. Magliozzi, D. B. Hanson and R. K. Amiet. “Aeroacoustics of flight vehicles: Theory and practice. Volume 1: Noise sources.” NASA Technical Report, Hampton, VA, 1991.
- [20] M. J. Kingan. “Open rotor broadband interaction noise.” J. Sound Vib. 332, 3956-3970, 2013.